

UC San Diego

UC San Diego Previously Published Works

Title

Mitochondria-dependent synthetic small-molecule vaccine adjuvants for influenza virus infection.

Permalink

<https://escholarship.org/uc/item/5xk4m8b4>

Journal

Proceedings of the National Academy of Sciences of the United States of America, 118(23)

ISSN

0027-8424

Authors

Sato-Kaneko, Fumi
Yao, Shiyin
Lao, Fitzgerald S
et al.

Publication Date

2021-06-01



DOI

10.1073/pnas.2025718118

Peer reviewed



Mitochondria-dependent synthetic small-molecule vaccine adjuvants for influenza virus infection

Fumi Sato-Kaneko^a, Shiyin Yao^a, Fitzgerald S. Lao^a, Jason Nan^a, Jonathan Shpigelman^a, Annette Cheng^a, Tetsuya Saito^a, Karen Messer^b, Minya Pu^b, Nikunj M. Shukla^a, Howard B. Cottam^a, Michael Chan^a, Anthony J. Molina^c, Maripat Corr^c, Tomoko Hayashi^{a,1} , and Dennis A. Carson^{a,1} 

^aMoore's Cancer Center, University of California San Diego, La Jolla, CA 92093-0809; ^bDepartment of Family Medicine and Public Health, University of California San Diego, La Jolla, CA 92093-0901; and ^cDepartment of Medicine, University of California San Diego, La Jolla, CA 92093-0656

Contributed by Dennis A. Carson, April 30, 2021 (sent for review December 14, 2020; reviewed by David J. Dowling and Jay A. Nelson)

Vaccine adjuvants enhance and prolong pathogen-specific protective immune responses. Recent reports indicate that host factors—such as aging, pregnancy, and genetic polymorphisms—influence efficacies of vaccines adjuvanted with Toll-like receptor (TLR) or known pattern-recognition receptor (PRR) agonists. Although PRR independent adjuvants (e.g., oil-in-water emulsion and saponin) are emerging, these adjuvants induce some local and systemic reactivity. Hence, new TLR and PRR-independent adjuvants that provide greater potency alone or in combination without compromising safety are highly desired. Previous cell-based high-throughput screenings yielded a small molecule 81 [*N*-(4-chloro-2,5-dimethoxyphenyl)-4-ethoxybenzenesulfonamide], which enhanced lipopolysaccharide-induced NF- κ B and type I interferon signaling in reporter assays. Here compound 81 activated innate immunity in primary human peripheral blood mononuclear cells and murine bone marrow-derived dendritic cells (BMDCs). The innate immune activation by 81 was independent of TLRs and other PRRs and was significantly reduced in mitochondrial antiviral-signaling protein (MAVS)-deficient BMDCs. Compound 81 activities were mediated by mitochondrial dysfunction as mitophagy inducers and a mitochondria specific antioxidant significantly inhibited cytokine induction by 81. Both compound 81 and a derivative obtained via structure–activity relationship studies, 2F52 [*N*-benzyl-*N*-(4-chloro-2,5-dimethoxyphenyl)-4-ethoxybenzenesulfonamide] modestly increased mitochondrial reactive oxygen species and induced the aggregation of MAVS. Neither 81 nor 2F52 injected as adjuvants caused local or systemic toxicity in mice at effective concentrations for vaccination. Furthermore, vaccination with inactivated influenza virus adjuvanted with 2F52 demonstrated protective effects in a murine lethal virus challenge study. As an unconventional and safe adjuvant that does not require known PRRs, compound 2F52 could be a useful addition to vaccines.

NF- κ B | mitochondrial reactive oxygen species | mitochondrial stress | vaccine adjuvant | influenza virus

Vaccine adjuvants enhance the immunogenic properties of antigens to enable enhanced and prolonged protective immune responses. Defined ligands for the pattern recognition receptors (PRRs)—including Toll-like receptors (TLRs), NOD-like receptors (NLRs), RIG-I like receptors (RLR), and stimulator of interferon genes (STING)—have been developed as adjuvants (1, 2). Although PRR-targeting adjuvants are well-tolerated and show promising protective efficacy, vaccination effectiveness is influenced by host factors causing variance in PRR signaling (e.g., aging, pregnancy, or genetic polymorphisms) (3). In the elderly population, activation of TLR signaling pathways is dysregulated, causing impaired activation or constant low-level activation, thereby reducing immune responses (4). Pregnant women are another vulnerable population where immunologic mechanisms that prevent fetal rejection can also lower the maternal response to vaccination. In addition to physiologic factors, genetic polymorphisms, particularly in TLRs and their adaptor proteins, have been reported to reduce responses to measles, meningococcal, and cytomegalovirus glycoprotein B vaccines (3, 5–7). To overcome variations in vaccine

responses by these and other host considerations, adjuvants independent of known PRR should be reevaluated for vaccine development.

Saponin and oil emulsions are TLR-independent vaccine adjuvants that have been recently approved by the Food and Drug Administration (FDA) (8, 9). Saponin adjuvants, including QS-21, induce strong humoral and T cell responses, and are FDA-approved for malaria and shingles vaccines (8–11). Saponin can disrupt the cell membrane, causing cytotoxicity, which can be reduced by proper formulation within liposomes or emulsions (12). The vaccines adjuvanted with QS-21 sometimes cause systemic adverse effects, including flu-like symptoms, fever, and malaise (13, 14). Oil-in-water adjuvants, including MF59 and AS03, are efficacious, but are also inflammatory in some recipients, inducing local swelling, pain, and fever (14–16). Therefore, new TLR-independent adjuvants with minimal if any local reactions are highly desirable.

To seek additional adjuvants that would act independently or as a coadjuvant to enhance the response to monophosphoryl lipid A (MPLA) (9, 17), an FDA-approved TLR4 agonist, we previously performed a high-throughput screening (HTS) using interferon (IFN)-stimulated response element (ISRE) reporter cells. Compound 81

Significance

Effective vaccine strategies are needed to overcome genetic, physiologic, or age-related deficits in immune responses relevant to vulnerable populations. Vaccine adjuvants that overcome these variants and do not compromise safety are highly desirable. We identified a synthetic small-molecule compound 81 [*N*-(4-chloro-2,5-dimethoxyphenyl)-4-ethoxybenzenesulfonamide] and its derivative 2F52 [*N*-benzyl-*N*-(4-chloro-2,5-dimethoxyphenyl)-4-ethoxybenzenesulfonamide] as activators of innate immunity via mitochondrial stress pathways, circumventing classic pathogen-recognition receptors. Neither 81 nor 2F52 as adjuvants caused local or systemic toxicity in mice after injection. Moreover, in a mouse influenza challenge study, compound 2F52 demonstrated protective effects when used with inactivated virus. Thus, compound 2F52, acting through an unconventional pathway to stimulate innate immunity, could be a useful synthetic adjuvant to enhance current and future vaccines.

Author contributions: F.S.-K., M. Corr, T.H., and D.A.C. designed research; F.S.-K., S.Y., F.S.L., J.N., J.S., A.C., T.S., and A.J.M. performed research; N.M.S., H.B.C., and M. Chan contributed new reagents/analytic tools; F.S.-K., K.M., M.P., M. Corr, and T.H. analyzed data; and F.S.-K., M. Corr, T.H., and D.A.C. wrote the paper.

Reviewers: D.J.D., Boston Children's Hospital; and J.A.N., Oregon Health & Science University.

The authors declare no competing interest.

Published under the [PNAS license](#).

¹To whom correspondence may be addressed. Email: thayashi@ucsd.edu or dcarson@ucsd.edu.

This article contains supporting information online at <https://www.pnas.org/lookup/suppl/doi:10.1073/pnas.2025718118/-DCSupplemental>.

Published June 2, 2021.

[*N*-(4-chloro-2,5-dimethoxyphenyl)-4-ethoxybenzenesulfonamide] that belonged to bis-aryl sulfonamide scaffold was identified as a low molecular weight compound that prolonged activation of ISRE induced by type I IFN (18) and was also found to enhance lipopolysaccharide (LPS)-induced NF- κ B responses (19). Further structure–activity relationship (SAR) studies identified the sites critical for immune-stimulatory properties of derivatives of **81**. Unlike most PRR ligands, these compounds can be easily synthesized in one to two synthetic steps from readily available commercial reagents. Additionally, compound **81**, when used as a coadjuvant with MPLA, showed significant enhancement in antigen-specific immunoglobulin responses compared to MPLA alone (19).

This study examines the mechanisms that lead to the downstream signaling pathways and efficacy of the compound **81** scaffold (bis-aryl sulfonamide) as a vaccine adjuvant. We demonstrate that compound **81** and its derivative **2F52** [*N*-benzyl-*N*-(4-chloro-2,5-

dimethoxyphenyl)-4-ethoxybenzenesulfonamide] increase mitochondrial stress associated with mitochondrial reactive oxygen species (mtROS) release, enhancing mitochondrial antiviral-signaling protein (MAVS)-dependent cytokine production, independent of known PRRs and inflammasomes. When used as an adjuvant with inactivated influenza A virus (IIAV) in a murine lethal influenza virus challenge model, the lead compound **2F52** protects mice from a lethal infection.

Results

Compound 81 Broadly Enhances Gene Expression Involved in Innate Immune Pathways. Compound **81** (Fig. 1A) was previously identified as a hit in two separate HTS, based upon its ability to prolong type I IFN-induced ISRE activation (18) (compound **3** in ref. 14) and to enhance LPS-induced NF- κ B activation (19) (compound **1** in ref. 15). To evaluate whether compound **81** could activate NF- κ B as a

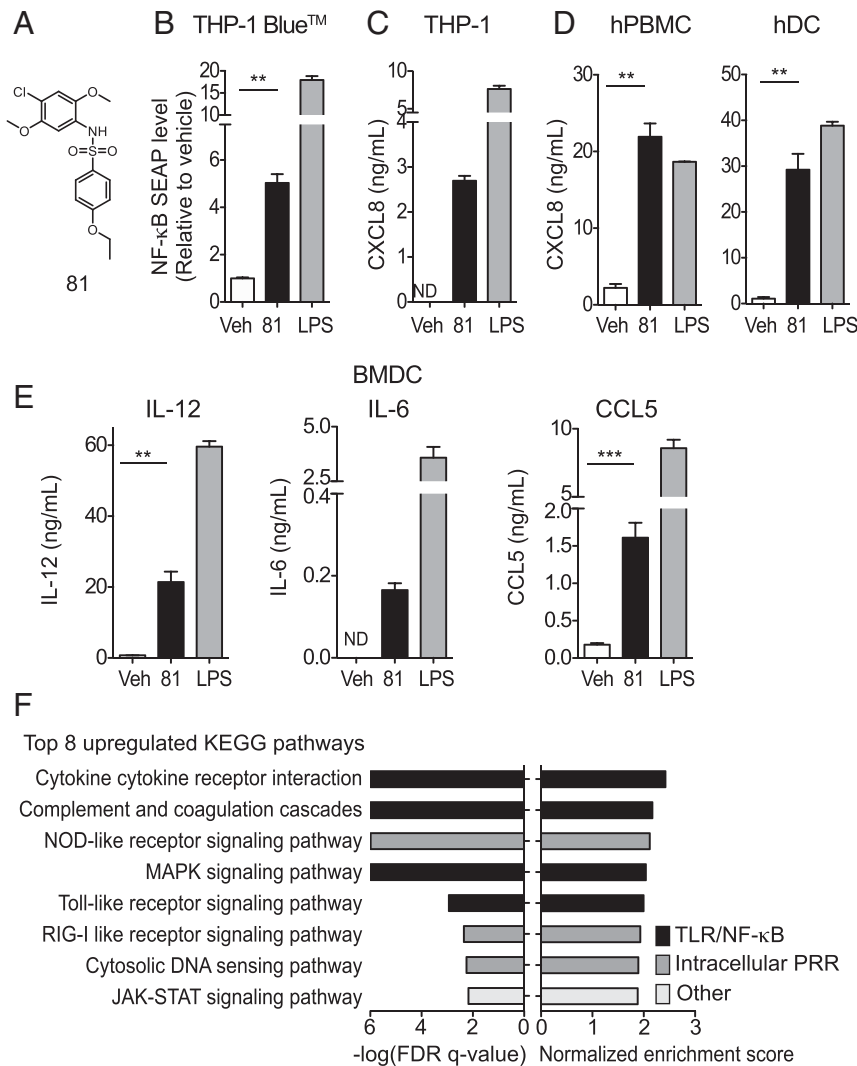


Fig. 1. Compound **81** broadly enhances genes involved in innate immune pathways. (A) Chemical structure of compound **81**. The innate immune stimulatory potency of compound **81** was examined in THP-1 Blue NF- κ B reporter cells (B), THP-1 cells (C), hPBMCs (D), and mouse BMDCs (E). Cells were cultured with 5 μ M **81** for 20 h and the culture supernatant was examined for NF- κ B-inducible SEAP protein and indicated cytokines/chemokines by ELISA. LPS (10 ng/mL for THP-1 Blue, THP-1 and hPBMC; 1 ng/mL for BMDC) served as a positive control. (B) NF- κ B-induced SEAP release from THP-1 Blue cells. (C) CXCL8 release from THP-1 cells. (D) CXCL8 release from primary hPBMCs and hDCs. (E) IL-12, IL-6, and CCL5 secretion from mouse BMDCs. (B–E) Bars represent means \pm SD of three replicated wells of cells. The experiment is representative of three independent experiments with similar results. ** P < 0.01, *** P < 0.0001, two-tailed unpaired t test with Welch’s correction. ND, below detection level. (F) Top eight up-regulated pathways in the GSEA of RNA-seq data. RNA-seq was performed with THP-1 cells treated for 5 h with 5 μ M **81** or vehicle. $-\log$ (FDR q -value) (Left) and normalized enrichment score (Right) are shown. Detailed procedures and results are in *Materials and Methods* (see also *SI Appendix*, Fig. S1 and Table S2).

single agent, THP-1 NF- κ B reporter cells (THP1-Blue) or the parental THP-1 cells were incubated with **81** overnight. Compound **81** significantly augmented the release of NF- κ B inducible secreted embryonic alkaline phosphatase (SEAP) and CXCL8 (Fig. 1B and C), indicating that it activated the NF- κ B signaling pathway as a single agent. Compound **81** was also active in primary human peripheral blood mononuclear cells (hPBMCs) and human dendritic cells (hDCs), as it induced production of CXCL8 (Fig. 1D). Compound **81** also induced interleukin (IL)-6, IL-12, and CCL5 release from murine bone marrow-derived DCs (BMDCs) (Fig. 1E). Given the early promise of this compound, we tested it for human ether-a-go-go-related gene (hERG) encoded potassium ion (K⁺) channel inhibition, because hERG channel blockade can cause cardiac arrhythmias (20). The cell-based automated patch-clamp assay demonstrated that compound **81** at 10 μ M inhibited the tail current by $27 \pm 4.0\%$, while the known potassium channel inhibitor E-4031 showed 50% inhibition at 0.043 μ M (IC₅₀ = 0.043 μ M) (SI Appendix, Table S1), suggesting that the potency of **81** to inhibit hERG potassium channels is low.

To explore the mechanisms of innate immune activation by compound **81**, transcriptomes of THP-1 cells treated with compound **81** or vehicle were compared by RNA-sequencing (RNA-seq) analyses. Gene set enrichment analyses (GSEA) using Kyoto Encyclopedia of Genes and Genomes (KEGG) revealed that the genes up-regulated by **81** were highly enriched for the PRR innate immune pathways (Fig. 1F). The TLR/NF- κ B related pathways included the “cytokine–cytokine receptor interaction,” “complement and coagulation cascades,” “MAPK signaling,” and “TLR signaling” blocks (Fig. 1F, black). The intracellular PRR pathways were identified as “NLR signaling,” “RLR signaling,” and “cytosolic DNA-sensing pathway” (Fig. 1F, dark gray, and SI Appendix, Fig. S1 and Table S2). Since kinases are often involved in regulating inflammatory pathways, compound **81** was screened by a cell-free active site-directed competition binding assay (KINOMEscan, Eurofins DiscoverX Corp.). Compound **81** did not inhibit the binding of the kinases in the panel to their known ligand (listed in SI Appendix, Table S3). However, there remains a possibility that **81** could indirectly interact with those kinases or affect their function through other molecules in intact cells.

Innate Immune Activation by **81 Is Mediated by MAVS and Not MyD88, TRIF, or STING.** The RNA-seq data indicated that many genes involved in PRR signaling are up-regulated by compound **81**. PRR signaling pathways are regulated via adaptor proteins: 1) TLR signaling utilizes two main adaptor proteins, myeloid differentiation primary response 88 (MyD88) and TIR domain-containing adaptor protein-inducing IFN- β (TRIF) (21), and 2) the cytosolic PRRs (e.g., RLRs) are regulated by STING and MAVS (22). Therefore, we examined whether the mechanism of action for **81** required these adaptor proteins. BMDCs generated from WT, *Myd88*^{-/-}, and *Ticam1*^{lps/lps} (TRIF mutant) mice were incubated with **81**, and the release of IL-12 and CCL5, which are established downstream targets of MyD88 and TRIF, respectively (SI Appendix, Fig. S2A), were evaluated by ELISA. Deficiencies in MyD88 or TRIF did not impact the induction of their respective downstream cytokines (Fig. 2A and B). Concordantly, experiments using HEK-Blue hTLR cells indicated that TLR2, TLR3, TLR4, TLR5, TLR7, TLR8, and TLR9 were not activated by **81** (SI Appendix, Fig. S3A).

We next analyzed whether the adaptor proteins for intracellular PRR signaling were involved in cytokine/chemokine release by **81**, using *Tmem173*^{-/-} (STING-deficient) and *Mavs*^{-/-} BMDCs. The lack of STING did not attenuate cytokine induction by **81** (Fig. 2C and SI Appendix, Fig. S2B). Because STING ligands behave differently with mouse and human cells due to the distinct structural differences between murine and human STING (23, 24), we evaluated whether compound **81** stimulated human STING. The assay using a STING knockout (KO) reporter cell line (THP-1-

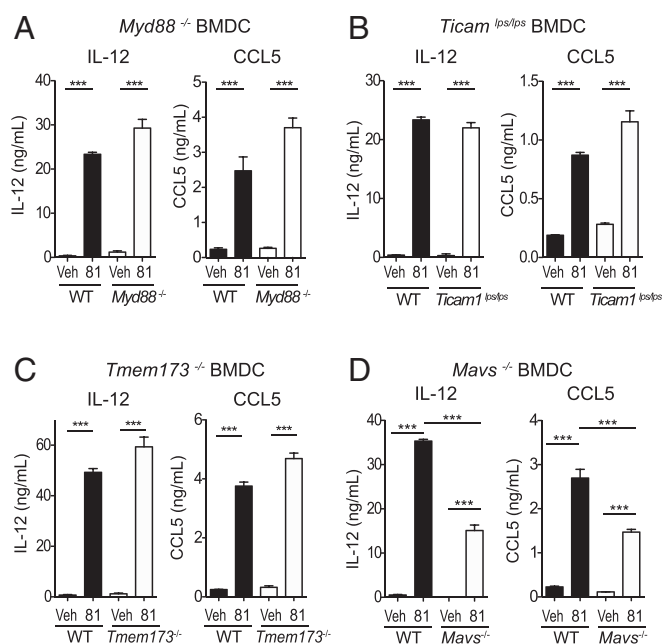


Fig. 2. MAVS is involved in innate immune activation by compound **81**. BMDCs prepared from WT, *Myd88*^{-/-} (A), *Ticam1*^{lps/lps} (TRIF mutant) (B), *Tmem173*^{-/-} (STING-deficient) (C), and *Mavs*^{-/-} (D) mice were stimulated with 5 μ M **81** overnight and the levels of IL-12 and CCL5 in the culture supernatant were measured by ELISA. Bars represent means \pm SD of three replicated wells of cells. ****P* < 0.0001, one-way ANOVA with Bonferroni's post hoc test. Data are representative of three independent experiments with similar results.

Dual KO-STING cell) showed that the immune activation induced by **81** was not dependent on human STING (SI Appendix, Fig. S4).

On the other hand, *Mavs*^{-/-} BMDCs treated with compound **81** released significantly lower levels of IL-12 and CCL5 compared to WT BMDCs (by 57% and 45%, respectively) (Fig. 2D). Of note, the cytokine levels induced by various PRR agonists in *Mavs*^{-/-} BMDCs were similar to those in WT BMDCs (SI Appendix, Fig. S2C), suggesting that MAVS deficiency does not nonspecifically interfere with other PRR pathways. Further experiments using reporter cell lines indicated that innate immune activation by **81** was not dependent on RIG-I, MDA5, NOD1, or NOD2 (SI Appendix, Fig. S3B–F). Taken together, these results demonstrate that MAVS plays an important role in the innate immune activation by **81**.

Compound **81 Induces Mitochondrial Stress Responses Involved in Cytokine Release.** MAVS is located on the mitochondrial outer membrane and recent studies have indicated that mitochondrial stressors can activate PRR pathways “downstream” of the various receptors (25–28). Thus, we studied whether compound **81** might alter mitochondrial integrity using MitoTracker red, which stains mitochondria in a membrane potential-dependent manner. The mitochondrial membrane potential ($\Delta\Psi$ m) in **81**-treated THP-1 cells was decreased by 34%, compared to that of vehicle-treated cells (Fig. 3A). This effect was mirrored by decreased mitochondrial basal respiration and ATP-linked respiration after incubation with **81**, as measured by Seahorse XFe96 (Fig. 3B). Stressed mitochondria are removed by mitophagy, a degradation mechanism related to autophagy, to maintain mitochondrial homeostasis in cells (29, 30). Therefore, we examined whether mitophagy inducers, urolithin A (UA) and 1,4-[4-4'-Bis-{[4-(dimethylamino)pyridinium-1-yl]methyl}diphenyl]butane dibromide (MN58b), inhibited cytokine induction by **81** (31, 32). Pretreatment with UA or MN58b reduced the levels of CXCL8 released by **81** stimulated THP-1 cells (Fig. 3C and SI Appendix, Fig. S5A), and the levels of IL-12

produced by **81** treated BMDCs (Fig. 3D and *SI Appendix, Fig. S5B*). These findings indicate that compound **81** induces mitochondrial stress, which in turn activates innate immune cascades.

Compound 81 Increases mtROS, Thereby Activating the MAVS Signaling Pathway. Elevated mitochondrial stress promotes assembly of inflammasomes, enhancing release of proinflammatory cytokines (e.g., IL-1 β and IL-18) (33–35). To test whether compound **81** promoted inflammasome activation, thereby enhancing cytokine release, BMDCs were incubated with compound **81** in the presence and absence of a pan-caspase inhibitor zVAD-FMK. The levels of IL-1 β detected by ELISA after **81** treatment were not diminished by treatment with zVAD-FMK, suggesting low levels of caspase independent release (*SI Appendix, Fig. S6*). The results suggest that the effect of **81** on inflammasome activation does not play a primary role in its cytokine induction.

We next studied whether induction of mitochondrial stress by **81** was associated with the release of mtROS using a superoxide indicator MitoSOX. The intracellular levels of mtROS were increased by compound **81** in a titration-dependent manner (Fig. 4A). Several studies have shown that elevated mtROS levels induces activation and aggregation of MAVS, leading to nuclear translocation of NF- κ B and IFN regulatory factors (IRFs) and subsequent transcription of innate immune mediators (36–38). We thus examined whether **81** could increase MAVS aggregation using A549 cells by semidenaturing electrophoresis and immunoblotting. High molecular weight MAVS agglomeration was modestly increased by **81** treatment, consistent with aggregation (Fig. 4B). Of note, phosphorylation of both NF- κ B p65 and IRF3, which are downstream signaling molecules of MAVS activation, were induced by **81** treatment, as assessed by immunoblot analysis (Fig. 4C). To further evaluate whether mtROS was involved in the innate immune responses

induced by **81**, THP-1 cells were pretreated with a mitochondria-targeted antioxidant MitoTEMPO. MitoTEMPO significantly diminished **81**-induced CXCL8 release (Fig. 4D). Collectively, these data indicate that mitochondria–mtROS–MAVS largely contribute to the innate immune activation by **81**.

Derivative 2F52 Induces mtROS- and MAVS-Dependent Cytokines.

The above results showed that mitochondrial stress contributed to compound **81**-induced immune responses. We further explored this activity using a chemical approach by examining eight derivatives of compound **81** from a prior SAR study for induction of mtROS levels (19), and ranked these compounds by mtROS levels (Table 1 and *SI Appendix, Fig. S7*). Among these compounds, only **2F52** (Fig. 5A), in addition to **81**, significantly increased mtROS generation compared to vehicle (152% of vehicle) (Table 1). Compound **2F52** induced CXCL8 production in THP-1 cells and the effect was diminished by MitoTEMPO (Fig. 5B) and mitophagy inducers (UA and MB58b) in a titration-related fashion (Fig. 5C). This inhibitory effects by the mitophagy inducers were confirmed in BMDCs (Fig. 5D). Finally, the levels of IL-12 and CCL5 released by **2F52**-treated BMDCs were significantly reduced by MAVS deficient BMDCs (Fig. 5E). These data demonstrate that compound **2F52**, similar to **81**, induced mtROS-mediated immune responses, which were partially dependent on MAVS (*SI Appendix, Fig. S8*).

Compounds 81 and 2F52 Are Effective Adjuvants that Promote Adaptive Immune Responses.

The *in vitro* experiments indicated that compounds **81** and **2F52** activated innate immune responses via induction of mitochondrial stress in antigen-presenting cells (APCs) independent of known PRRs. Recent reports have shown that APC function is tightly regulated by mitochondria (39–41). Hence, we examined whether **81** and **2F52** enhanced antigen presentation to T cells. The flow cytometric analysis showed that both **81** and **2F52** increased the expression of CD40 and CD86 in BMDCs (Fig. 6A). To test whether **81** or **2F52**-treated BMDCs enhanced antigen-specific T cell proliferation, BMDCs were incubated with ovalbumin (OVA), and antigen-presenting function was evaluated by proliferation of CD4⁺ T cells transgenic for OVA_{323–339}-specific T cell receptors isolated from DO11.10 mice. After 3 d of coculture, DO11.10 CD4⁺ T cell proliferation was enhanced by **81**- or **2F52**-treated BMDCs, compared to that of DO11.10 CD4⁺ T cells cocultured with vehicle-treated BMDCs (*SI Appendix, Fig. S9A*). The presence of a mitophagy inducer, MN58b, decreased the proliferation of the DO11.10 CD4⁺ T cells (*SI Appendix, Fig. S9B*). These data indicate that **81** and **2F52** enhance the antigen-presenting function of BMDCs through a mechanism that included stressed mitochondria.

To further evaluate whether the promotion of APC function by **81** and **2F52** could translate to enhanced *in vivo* adjuvant effects, BALB/c mice were intramuscularly immunized with OVA plus compound (50 nmol per injection) on days 0 and 21, and intraperitoneally injected with OVA on day 39. Antigen-specific antibody levels on days 28 and 41 were assessed by ELISA (Fig. 6B and *SI Appendix, Fig. S10*). Anti-OVA IgG1 and IgG2a levels in the sera of the animals that received OVA adjuvanted with **81** or **2F52** were significantly higher than the levels from animals immunized without adjuvant, on both day 28 before the boost, and day 41 (Fig. 6C and *SI Appendix, Fig. S11*). Both **81** and **2F52** as adjuvants induced Th1- and Th2-associated responses as evidenced by increases in IgG2a and IgG1, which have been reported to be secondary markers of Th responses (Fig. 6B) (42, 43).

Compounds 81 and 2F52 Do Not Induce Local or Systemic Inflammation.

Excessive mtROS production has been associated with apoptosis and other forms of cell death (44, 45). However, flow cytometric analysis showed that neither **81** nor **2F52** triggered apoptosis in primary mouse BMDCs (*SI Appendix, Fig. S12A*). Correspondingly, lactate dehydrogenase (LDH) release from the cytoplasm of

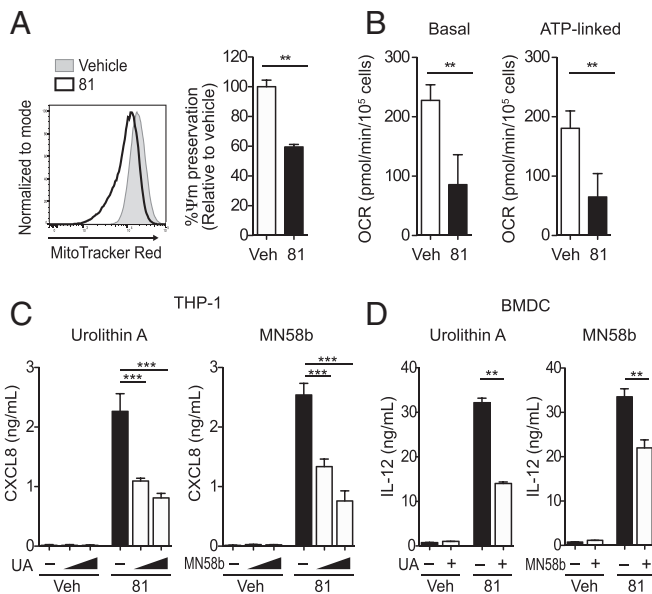


Fig. 3. Compound **81** induces mitochondrial stress responses involved in cytokine release. THP-1 cells (A–C) and BMDCs (D) were cultured with 5 μ M **81** for 20 h. (A) $\Delta\Psi$ m was assessed using MitoTracker FM red and the fluorescence intensity was evaluated by flow cytometry. Representative histograms and the mean fluorescence intensity (MFI) relative to vehicle are shown. (B) Oxygen consumption rate (OCR) (pmol/min/ 10^5 cells) was evaluated using Seahorse XF96. $**P < 0.01$, unpaired two-tailed *t* test with Welch's correction (A and B). (C) Mitophagy inducers UA (6.25 and 12.5 μ M) and MN58b (2.5 and 5 μ M) reduced CXCL8 release by **81**. $***P < 0.0001$, one-way ANOVA with Dunnett's post hoc test. (D) IL-12 secretion from BMDCs induced by **81** was decreased in the presence of UA (25 μ M) or MN58b (5 μ M). $**P < 0.01$, unpaired two-tailed *t* test with Welch's correction.

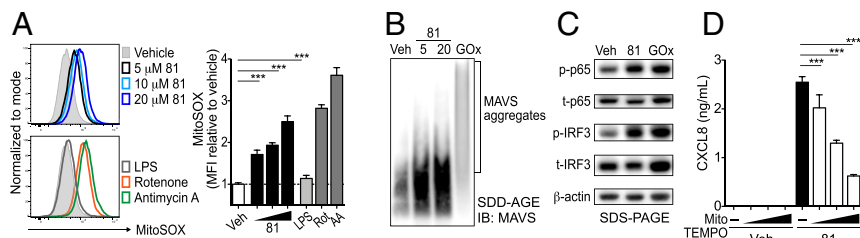


Fig. 4. Compound **81** increases mtROS activating the MAVS signaling pathway. (A) mtROS levels. THP-1 cells were incubated with **81** (5, 10, and 20 μ M), vehicle and LPS (10 ng/mL) for 3 h, followed by staining with MitoSOX. MFI of oxidized MitoSOX was evaluated by flow cytometry. Rotenone (Rot; 1 μ M) and antimycin A (AA; 1 μ M) for 30 min were used as positive controls. MFIs normalized to vehicle are shown. $***P < 0.0001$, one-way ANOVA with Dunnett's post hoc test. (B) MAVS aggregates in A549 cells assayed by SDD/AGE followed by immunoblot with anti-MAVS antibody. Cells were incubated for 4 h with **81** (5 and 20 μ M) and 1 U/mL glucose oxidase (GOx; positive control). (C) Immunoblot for phosphorylation of NF- κ B p65 and IRF3 from total cell lysates. A549 cells were treated with 5 μ M **81**, 0.02 U/mL GOx for 6 h. (D) Mitochondria-targeted ROS scavenger (superoxide scavenger, MitoTEMPO; 6.25, 25, and 100 μ M) suppressed CXCL8 production induced by **81**. $***P < 0.0001$, one-way ANOVA with Dunnett's post hoc test. Bars indicate means \pm SD. Data shown are representative of three independent experiments with similar results.

human THP-1 cells after **81** and **2F52** treatment, was less than that induced by LPS (SI Appendix, Fig. S12B), which is not a mtROS inducer (Fig. 4A). These experimental results indicated that neither **81** nor **2F52** triggered cell death at immunostimulatory concentrations.

Although TLR-independent adjuvants (e.g., the oil-in-water emulsion MF59, and various saponins) are effective in humans, they may induce local and systemic symptoms, including myalgias, malaise, and fever (13–15). Hence, local reactogenicity was examined 24 h following intramuscular injection of compounds **81** and **2F52** (Fig. 7A). Histologic analysis of muscles at the injection sites demonstrated that **81** and **2F52** induced minimal infiltration of monocytes and neutrophils compared to AddaVax (MF59). Necrosis and edema in the muscles was not observed in any treatment group (Fig. 7B). To evaluate systemic inflammation, sera were collected 2 and 24 h after injection and tested for CXCL1, IL-6, and C-reactive protein (CRP) as systemic inflammatory biomarkers (8). Compounds **81** and **2F52** did not induce elevated levels of CXCL1 or IL-6 in the sera (Fig. 7C) and induced minimal levels of CRP (Fig. 7D), whereas MPLA and AddaVax caused elevations of these biomarkers. To further evaluate morbidity after administration of compounds, mice were intraperitoneally injected with a maximum feasible dose of a liposomal formulation of **81** and **2F52** (100 mg/kg). No body-weight loss or altered behavior was noted in animals injected with the compounds (Fig. 7E). Collectively, these results indicate that compounds **81** and **2F52** do not induce local or systemic adverse effects.

Compound 2F52 Adjuvanted IIAV Protects Mice against Lethal Influenza Virus Challenge. To examine the adjuvant effects of **81** and **2F52** for influenza virus vaccine, a lethal challenge study of influenza virus in a mouse model was performed. BALB/c mice were intramuscularly vaccinated with IIAV [A/California/07/2009; (H1N1)pdm09] plus **81** or **2F52** and subsequently were intranasally challenged with a lethal dose (1×10^5 [$3 \times LD_{50}$] cell culture infectious doses [$CCID_{50}$] of virus per mouse) of the homologous influenza virus strain. The body weights and survival of the animals were monitored (Fig. 8A). The weight loss in the animals vaccinated with IIAV adjuvanted with **2F52** was significantly reduced over the observation period, compared to that in the mice given IIAV alone. (Fig. 8B). Mice immunized with inactivated virus adjuvanted with **2F52** showed 70% survival, while the vehicle group yielded only 30% survival ($P = 0.12$) (Fig. 8C), indicating that **2F52** was an effective adjuvant.

Discussion

Vaccines often rely on adjuvants that induce strong innate immune responses in order to obtain an adequate protective response. Although there have been recent advances in adjuvanted vaccines that overcome reduced immune responses in the elderly

for shingles and influenza, the adjuvants can generate local and systemic reactogenicity. These adverse effects can reduce compliance particularly if a second injection is needed. Accordingly, there is an unmet need to identify new safe adjuvants independent of TLRs or known PRRs for major infectious diseases. Here we have described synthetic adjuvants that activate innate immune responses independently of most known PRRs, reducing variance in vaccine efficacy based on host factors, such as age and genetic polymorphisms.

In the initial HTS, compound **81** emerged as a lead compound as it was able to enhance both ISRE and NF- κ B activation (18, 19). Based on these activities, **81** was suspected of being an innate immune activator. RNA-seq analysis confirmed that **81** treatment of THP-1 cells activated multiple signaling pathways associated with PRR stimulation. Screens using TLR reporter cells and KO BMDCs indicated that **81** was not an agonist of TLRs, RIG-1, or NOD1/2. Further testing of cells deficient in the major PRR adaptor proteins MyD88, TRIF, STING, and MAVS showed that compound **81**-induced IL-12 and CCL5 were significantly lower in *Mavs*^{-/-} BMDCs. As MAVS is located on mitochondrial outer membranes, we postulated that mitochondria mediate innate immune activation by compound **81**.

Recent studies have shown that mitochondria are critical regulators of innate immune activation by TLRs (46–48). Mitochondria play essential roles in activating innate immune responses as

Table 1. Compounds 81 and derivative 2F52 induce mtROS

Compound ID ^{*,†}		mtROS (% relative to vehicle) [‡]	
		Mean	\pm SEM
81	1	150.9**	10.2
2F52	46	151.6**	14.0
2B264	33	122.7	6.2
2B271	26	119.4	17.2
2B263	12	113.3	6.0
2F25	50	107.6	12.5
2F36	54	99.7	10.1
2F32	53	95.8	8.0
2F35	23	108.6	7.8
DMSO		100	

^{**} $P < 0.01$, one-way ANOVA with Dunnett's post hoc test.
^{*}Eight SAR derivatives and an inactive derivative 2F35 in the previous SAR study (first column).
[†]Corresponding compound ID in ref. 19 (second column).
[‡]mtROS induction relative to vehicle (100 = vehicle), was evaluated using MitoSOX. Means \pm SEM of three independent experiments.

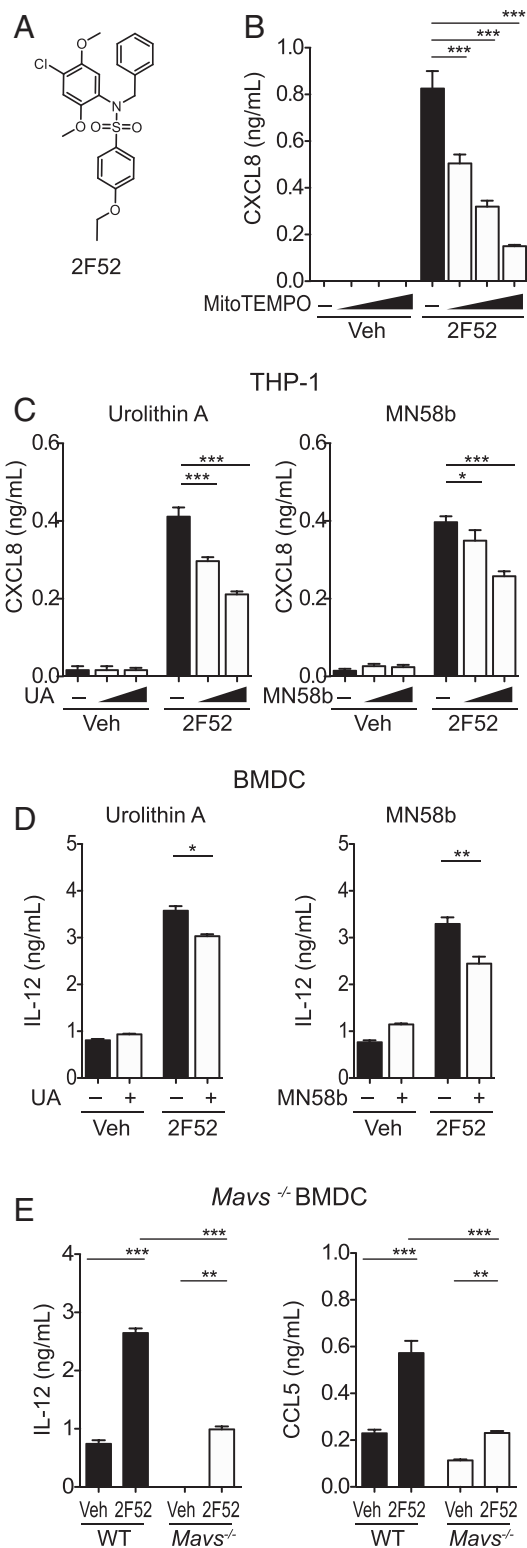


Fig. 5. Innate immune activation by 2F52 is associated with mitochondrial stress. (A) Chemical structure of compound 2F52. (B) CXCL8 level induced by 5 μ M 2F52 was suppressed by MitoTEMPO. (C and D) Mitophagy inducers UA and MN58b reduced cytokine release induced by 2F52. (C) THP-1 cells were preincubated with UA (6.25 and 12.5 μ M) or MN58b (2.5 and 5 μ M). After pretreatment with UA and MN58b, the cells were treated with 5 μ M 2F52 overnight. CXCL8 release from THP-1 cells was measured by ELISA. * P < 0.05, ** P < 0.01, *** P < 0.0001, one-way ANOVA with Dunnett's post hoc test (B and C). (D) IL-12 release from BMDCs by 2F52 was inhibited in the presence of UA (25 μ M) and MN58b (5 μ M). * P < 0.05, ** P < 0.01, two-tailed

“signaling hubs” (27, 28, 49). For example, the cGAS-STING or RIG-I/MDA5 pathways can be activated by aberrantly processed nuclear RNAs and DNA or double-stranded RNA (dsRNA) released from stressed mitochondria (25, 26, 50). Under stressed conditions, mitochondria release mtDNA and mtROS to regulate immune cell activation (34). mtDNA release can be sensed by cGAS-STING. However, our study using STING-deficient BMDCs and human STING KO reporter cells demonstrated that activation by **81** was not dependent on STING. The release of mtROS, oxidized mitochondrial proteins and lipids have also been implicated in these effects. In our study, **81** decreased $\Delta\Psi_m$ and increased mtROS release, which did not trigger cell death. The mitophagy inducers, UA and MN58b and mitochondria-specific antioxidant, MitoTEMPO significantly reduced cytokine release by **81**, indicating that immune-activating effects by **81** were attributable in part to mtROS generation (Figs. 3 and 4).

Stressed mitochondria can also activate MAVS-mediated antiviral signaling and NLRP3-mediated inflammasome assembly (33–37). MAVS senses intracellular dsRNA and triggers antiviral cascades via RIG-I–IRF3/7 (51). Our screens eliminated RIG-I as a significant intermediary or key target for **81**. However, virus-mediated MAVS aggregation is associated with transcription of NF- κ B and ISRE target genes, which is consistent with the original HTS data identifying compound **81** as activating ISRE and NF- κ B reporter cell lines and the RNA-seq data. Compound **81** induced modest levels of MAVS aggregation, which may be the mechanism of its ISRE and NF- κ B signaling activities.

To confirm that mtROS induction was functionally related to the adjuvant effects of this bis-aryl sulfonamide scaffold, eight SAR derivatives with different potencies for activation of the NF- κ B and ISRE pathways, were chosen for analysis (19). Only **81** and **2F52** induced significant mtROS release accompanied by cytokine production (Fig. 5 and Table 1). In this study the animals injected with **81** and **2F52** showed minimal local reactogenicity or systemic cytokine/chemokine induction compared to the animals injected with the TLR-independent adjuvants, MF59 (Fig. 7). In an influenza challenge model in mice, vaccination with inactivated virus adjuvanted with **2F52** effectively protected the animals from lethal influenza challenge, achieving 70% protection against virus challenge (Fig. 8). In vitro, **81** induced stronger immune activation than **2F52**, but in vivo the latter compound was a more effective adjuvant. The different potencies might be associated with the physical properties of these low molecular weight compounds that effect local retention and cell penetration. Further studies with formulation of the compounds in liposomes and oil-in-water emulsions will be necessary to optimize their efficacy.

In summary, two synthetic adjuvants, **81** and **2F52**, which act independently of known TLRs and PRRs, have been identified and characterized. In human monocytic THP-1 cells and in mouse BMDCs the compounds up-regulated genes involved in broad innate immune responses. The two adjuvants can be safely administered in mice. MAVS deficiency or attenuating mtROS using antioxidants or mitophagy inducers significantly reduced their innate immune activity. In influenza virus challenge studies, compound **2F52**-adjuvanted IIAV vaccine protected animals from lethal viral challenge. Compound **2F52** induced no local or systemic reactogenicity. Based upon the mechanism of action distinct from PRRs, ease of synthesis, and safety, compound **2F52** may be a promising candidate for further development as a vaccine adjuvant.

unpaired *t* test with Welch's correction. (E) IL-12 and CCL5 secretion from WT and *Mavs*^{-/-} BMDCs after overnight incubation with 5 μ M 2F52. ** P < 0.01, *** P < 0.0001, one-way ANOVA with Bonferroni's post hoc test (E). Bars indicate means \pm SD of triplicates. Data are representative of three independent experiments with similar results.

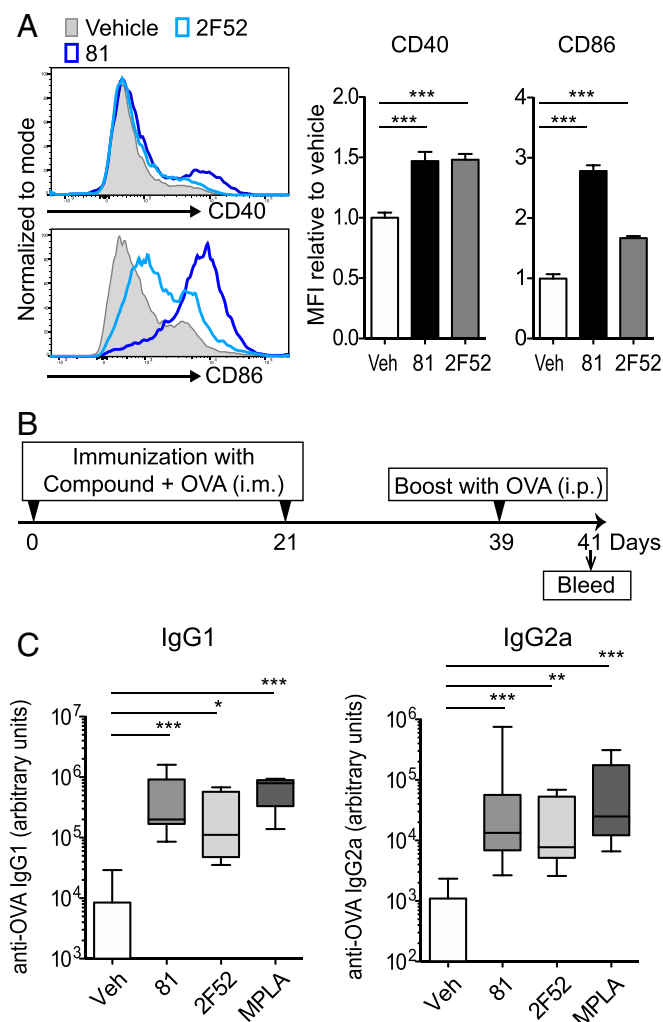


Fig. 6. Compounds **81** and **2F52** enhance expression of CD40 and CD86 and antigen-specific antibody induction. (A) Expression levels of costimulatory molecules CD40 and CD86 on BMDCs were enhanced by **81** and **2F52**. BMDCs were cultured with **81** or **2F52** overnight and the expression of CD40 and CD86 was examined by flow cytometry. MFI relative to vehicle is shown. Bars represent means \pm SD of three replicated wells. $**P < 0.01$, $***P < 0.0001$, one-way ANOVA with Dunnett's post hoc test. (B) Enhanced antigen specific antibody induction by compound plus OVA. BALB/c mice ($n = 8$ per group) were intramuscularly immunized with 50 nmol per injection **81** or **2F52** or 1 μ g MPLA plus 20 μ g per injection OVA on days 0 and 21, intraperitoneally boosted with 100 μ g per injection OVA on day 39 and bled on day 41. (C) OVA-specific IgG1 (Left) and IgG2a (Right) levels in sera are shown. In each box plot, the line within the box represents the median, the bounds are the upper and lower quartiles and the bars indicate minimum and maximum values. Bars represent means \pm SEM $*P < 0.05$, $**P < 0.01$, $***P < 0.0001$, Kruskal-Wallis test with Dunn's post hoc test comparison to vehicle. The pooled data from two independent experiments with similar results are shown.

Materials and Methods

Mice. Six- to 8-wk-old BALB/c, C57BL/6, B6129SF2/J, *Tmem173*^{-/-}, *Ticam1*^{lpsIIps}, *Mavs*^{-/-}, and DO11.10 mice were obtained from The Jackson Laboratories. *Myd88*^{-/-} mice were gifts from Shizuo Akira, Osaka University, Osaka, Japan, and were back-crossed more than 10 times to C57BL/6 mice. All animal experiments received prior approval by the University of California San Diego Institutional Animal Care and Use Committee.

The influenza challenge study was performed by the Institute for Antiviral Research of Utah State University using female 6-wk-old BALB/c mice from Charles River Laboratories. The challenge study was conducted in accordance with the approval of the Institutional Animal Care and Use Committee of

Utah State University. The work was done in the Association for Assessment and Accreditation of Laboratory Animal Care-accredited Laboratory Animal Research Center of Utah State University.

Cells and Reagents. THP-1 and A549 cells were purchased from the American Type Culture Collection and were cultured with RPMI and F-12K media, respectively, according to the provider's instructions. Human blood was obtained from the San Diego Blood Bank and hPBMCs were isolated using Ficoll-Paque Plus (GE Healthcare). Human peripheral blood immature DCs were purchased from Stemcell Technologies (#70041). BMDCs were generated as previously described (52, 53). For examining compounds in THP-1 cells and BMDCs, RPMI medium with 10% FBS supplemented with 100 U/mL penicillin and 100 μ g/mL streptomycin (without β -mercaptoethanol) was used. Nigericin were purchased from R&D Systems. Oligomycin, FCCP [Carbonyl cyanide 4-(trifluoromethoxy)phenylhydrazone], antimycin A, rotenone, MitoTEMPO [(2-(2,2,6,6-Tetramethylpiperidin-1-oxyl-4-ylamino)-2-oxoethyl)triphenylphosphonium chloride] and UA were obtained from Sigma Aldrich. MN58b was purchased from AOBIOS Inc. Compound **81** and its derivatives were synthesized as previously described (SI Appendix, Fig. S7) (19).

THP-1 Blue NF- κ B Cells and HEK-Blue hTLR Cells. The THP-1-Blue NF- κ B cell line and HEK-Blue TLR4/NF- κ B cells were purchased from InvivoGen (#thpnfkb and #hkb-htlr4). NF- κ B /SEAP (SEAPorter) HEK 293 cells for TLR2, TLR3, TLR5, TLR7, TLR8, or TLR9 was obtained from Imgenex. The assay was performed according to the manufacturer's protocols (19). TLR reporter cells were treated with corresponding agonist for 20 h: Pam3CSK4 (TLR2), Poly(I:C) (TLR3), LPS (TLR4), FLA-ST (TLR5), 1V136 (SM360320, TLR7) (54, 55), R848 (TLR8), or ODN2006 (TLR9); 0.5% DMSO was used as the vehicle.

hERG Safety Assay. Effects of compound **81** (0.1, 1, and 10 μ M) on hERG human potassium ion channel was performed using cell-based antagonist patch assay (automated patch-clamp assay) by Eurofin Pharma Discovery Service (Eurofin Panlabs). E-4031 was used as a positive control. The amplitude of hERG potassium channel tail currents $<50\%$ of the control peak tail current were considered channel inhibition.

Kinase Screening. The protein kinase selectivity of compound **81** (5 μ M) was tested in a high-throughput binding assay (KINOMEScan, Eurofins DiscoverX) against a panel of 97 kinases (<https://www.discoverx.com/services/drug-discovery-development-services/kinase-profiling/kinomescan>). The binding was calculated as follows: %Ctrl = (test compound signal-positive control signal)/(negative control signal-positive control signal) \times 100. Negative control = DMSO (100%Ctrl) and positive control = control compound (0%Ctrl). Less than 35% of control kinase activity was considered to be active inhibition.

RIG-I/MDA5, NLR, and STING Ligand Screening. Compound **81** was submitted to InvivoGen for RLR and NLR ligand screening and the assays were performed by InvivoGen (<https://www.invivogen.com/custom-trl-screening>). For RIG-I and MDA5 ligand screening, 5 μ M **81** was tested in HEK293 cells expressing hRIG-I or MDA5 genes. The secreted luciferase reporter protein was under the control of an IRF inducible promoter. Positive controls included Poly(I:C)/LyoVec, 5'pppdsRNA/LyoVec or hIFN α . The HEK293/Null cell line served as the negative control for comparison. The NLR activation screens used the SEAP reporter cell lines, HEK-Blue-hNOD1 and -hNOD2. C12-iE-DAP (hNOD1 ligand) and L18-MDP (hNOD2 ligand) were used as positive controls. Compound **81** was tested on a STING KO reporter cell line (THP-1-Dual KO-STING cell) and the parental cell line (THP-1 Dual cells), which express a reporter gene with IRF-inducible Lucia luciferase. Human STING agonists 10 μ g/mL c-di-AMP and 10 μ g/mL 2'3'-cGAMP, and 1,000 U/mL IFN β (negative control) were also tested on both cell lines.

Cytokine Assays. THP-1 cells (10^5 cells), hPBMCs (10^5 cells), hDCs (2×10^5 cells) or BMDCs (2×10^5 cells) were plated in 200 μ L per well in 96-well plates and cultured with 5 μ M compound or 0.5% DMSO (vehicle) for 20 h. For treatments with the mitochondria specific superoxide scavengers (MitoTEMPO) and the mitophagy inducers (UA and MN58b) (31, 32), cells were preincubated with each chemical, followed by stimulation with **81** or **2F52** (1-h preincubation with UA and MN58b, 3 h with MitoTEMPO). The concentrations of other stimuli and treatment periods are detailed in each figure legend. The culture supernatant was tested for cytokine levels by ELISA (human CXCL8 for THP-1 cells and mouse IL-12p40/p70, IL-6, and CCL5 for BMDCs). Antibodies and reagents used in these ELISAs are listed in SI Appendix, Table S4.

Evaluation of Mitochondrial Integrity. THP-1 cells were cultured with 5 μ M compounds for 20 h (5×10^5 cells/mL) and stained for mitochondrial

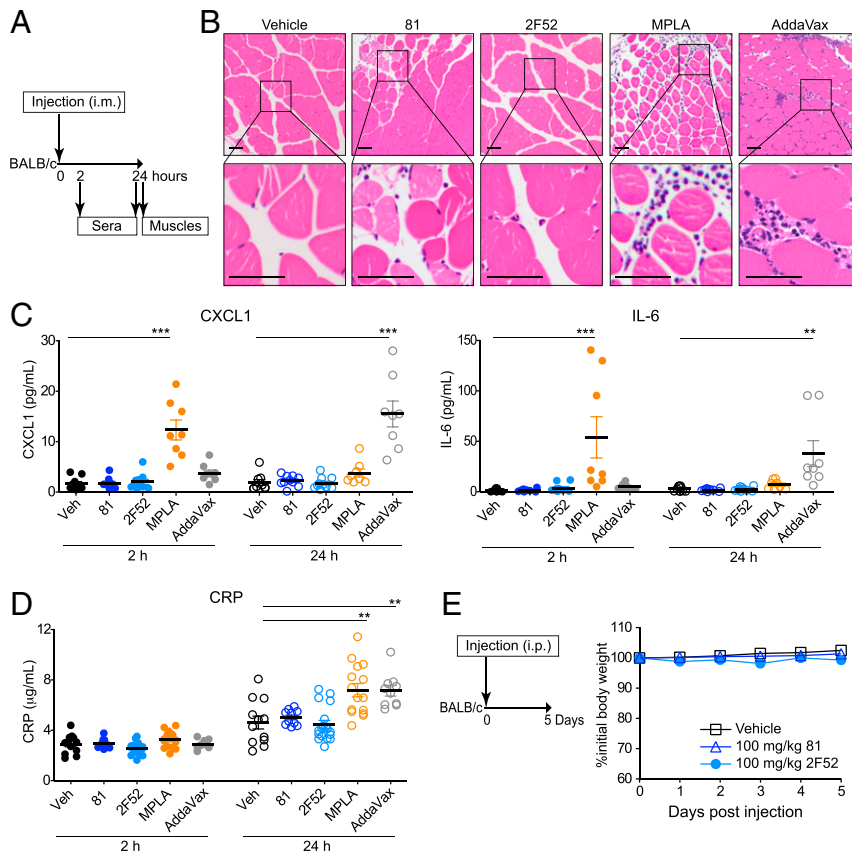


Fig. 7. Assessment of local and systemic inflammation following intramuscular injection of compounds. (A) BALB/c mice ($n = 8$ to 10 per group) were injected in the gastrocnemius muscle with **81**, **2F52** (50 nmol per injection), MPLA (10 μ g per injection), or AddaVax (25 μ L per injection) in a volume of 50 μ L and were bled at 2 and 24 h postinjection. Muscles at the injected sites were harvested at 24 h postinjection. (B) Histological analysis of injected muscles by H&E staining. The *Insets* are shown at higher magnification in the lower panels ($20\times$ and $40\times$ objectives were used). (Scale bars, 50 μ m.) (C) CXCL1 and IL-6 levels in the sera were evaluated using multiplex cytokine Luminex assay. (D) CRP levels in sera collected at 2 and 24 h ($n = 10$ to 18 per group) were assessed by ELISA. (C and D) Bars represent means \pm SEM, $***P < 0.01$, $***P < 0.0001$, Kruskal–Wallis test with Dunn’s post hoc test (comparison to vehicle). The pooled data of two independent experiments are shown. (E) Assessment of maximum feasible dose. Mice were intraperitoneally administered with 100 mg/kg (0.27 mmol/kg) **81** and 100 mg/kg (0.22 mmol/kg) **2F52** and body weight was monitored. There was no observable behavioral change in animals throughout 2 h post-administration. There was no statistical significance difference by one-way ANOVA with Dunnett’s post hoc test.

polarization using MitoTracker FM red according to the manufacturer’s instructions (Thermo Fisher Scientific, #M22425). In brief, after washing cells with prewarmed fresh media, prewarmed 100 nM MitoTracker red was added and incubated for 30 min at 37 $^{\circ}$ C followed by washing with prewarmed media. Cells were stained with DAPI before data acquisition. The intensity of MitoTracker red was evaluated by flow cytometry (MACSQuant Analyzer 10, Miltenyi Biotec) and the DAPI^{hi} cells were gated out and considered to be dead. Since MitoTracker red stains mitochondria in a membrane potential-dependent manner, the fluorescence intensity of this dye corresponds to the preserved mitochondrial membrane potential. For mitochondrial respiration, a Mito Stress Test was performed using Seahorse XF96 according to the manufacturer’s protocol (Agilent). Ninety-six-well plates were coated with poly-D-lysine for 2 h. THP-1 cells (10^5 cells per well) were preincubated for 3 h to rest, then 5 μ M **81** or 0.5% DMSO (vehicle) was added. The cells were assayed for oxygen consumption during injections with 1 μ M oligomycin, 1.5 μ M FCCP, 1 μ M antimycin A/ 1 μ M rotenone.

mtROS Assessment. For mtROS, MitoSOX Red was used to assess mitochondrial superoxide in live cells according to manufacturer’s instructions (Thermo Fisher Scientific, #M36008). Briefly, THP-1 cells were treated with 0.5% DMSO (vehicle), 5 μ M compound, LPS (10 ng/mL) for 3 h, rotenone (1 μ M), or antimycin A (1 μ M) for 30 min as positive controls. The cells were then stained with 5 μ M MitoSOX red for 15 min at 37 $^{\circ}$ C followed by washing with HBSS. The fluorescence intensity of the oxidized dye was then measured by flow cytometry.

Detection of MAVS Aggregates. A549 cells were treated with 5 μ M **81**, 1 U/mL glucose oxidase (GOx; positive control), or 0.5% DMSO (vehicle) for 4 h. MAVS

aggregates in the cells were assessed by semidenaturing detergent agarose gel electrophoresis (SDD/AGE) followed by immunoblotting, as previously described (36, 56). Estimated protein concentrations of the cell lysates were determined using Pierce BCA protein assay kit (Thermo Fisher Scientific). Fifteen micrograms of protein per sample was mixed with bromophenol blue (final concentration of 0.0025%) and then loaded on a vertical 1.5% agarose gel with 0.1% SDS. After electrophoresis in running buffer ($1\times$ TBE and 0.1% SDS), protein was transferred onto Immobilon-P PVDF membranes (EMD Millipore). The membrane was probed with anti-human MAVS antibody ($1:1,000$; Cell Signaling Technology) overnight.

Immunoblots. A549 cells (5×10^5 cells per 60 -mm dish) were treated with 5 μ M compound **81**, 0.02 U/mL GOx, or 0.5% DMSO (vehicle) for 6 h. Cells were lysed with PhosphoSafe extraction reagent (EMD Millipore, #71296) supplemented with protease inhibitor mixture (Roche) and 0.1% SDS (Sigma). Ten micrograms of reduced and denatured protein per sample was then separated by gel electrophoresis using NuPage 4 to 12% Bis-Tris Gel (Thermo Fisher Scientific) and transferred onto Immobilon-P PVDF membranes. Membranes were blocked with 5% nonfat milk in 0.1% Tween-20 Tris-buffered saline (TBST) and subsequent washes were done in TBST. Membranes were probed with antibodies for NF- κ B p65, p-NF- κ B p65 (65 kDa), p-IRF3, IRF3 (45 to 55 kDa), and β -actin (45 kDa) followed by secondary antibodies. Details for antibodies are shown in *SI Appendix, Table S5*.

RNA-Seq. THP-1 cells were incubated for 5 h with vehicle control or 5 μ M **81** in triplicate and then RNA was isolated using Quick-RNA Miniprep kit according to manufacturer’s instructions (Zymo Research). High-throughput RNA-seq was

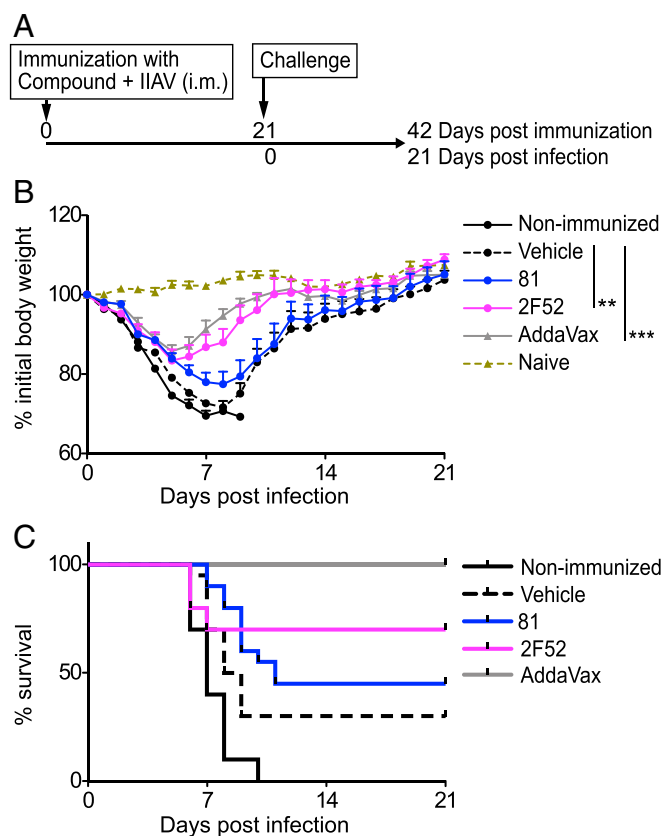


Fig. 8. Compound 2F52 protects against lethal influenza virus challenge. (A) Experimental protocol of the influenza challenge model. BALB/c female mice were intramuscularly immunized with IIAV A/CA/07/2009 (H1N1pdm) plus **81** or **2F52** (100 nmol per injection) or AddaVax (25 μ L per injection). After 21 d, mice were intranasally challenged with influenza A/CA/04/2009 (H1N1pdm) virus ($n = 10$ to 20 mice per group). (B) Percent initial body weights. Bars indicate means \pm SEM; $**P < 0.01$, $***P < 0.0001$, one-way ANOVA with Dunnett's post hoc test. (C) Percent survival of mice. Compound **81** vs. vehicle, $P = 0.13$; **2F52** vs. vehicle, $P = 0.12$; AddaVax vs. vehicle, $**P < 0.01$, by log-rank test.

performed by the sequencing core at La Jolla Institute for Allergy and Immunology (San Diego, CA). Reads were mapped using TopHat with hg19 annotation; reads mapped to tRNA/rRNA, adapters, and intergenic regions were filtered. HTseq was used for read count quantification. Genes were filtered if more than two-thirds of the samples had counts < 10 . Raw counts were then upper-quantile normalized and used as expression values in the following analysis. Linear models for microarray (Limma, using R-limma package) were used to compare groups regarding \log_2 expression values. The Benjamini-Hochberg procedure was applied to control the false-discovery rate (FDR). A gene was considered significantly changed if $FDR < 0.05$. If \log_2 fold-change in expression for a test compound vs. control was greater than 0, it was said to be up-regulated; otherwise, it was down-regulated. In addition, \log_2 fold-changes between two groups (**81** vs. vehicle) for all the genes included in the analysis set were extracted and preranked for GSEA (using GSEA v3.0 from the Broad Institute). Enrichment in KEGG pathways (c2.cp.kegg.v6 from Broad Institute) was examined. For each gene set, the number of expressed genes in the analysis data set was calculated along with enrichment score, the P value and q -value for testing enrichment significance, and the number of core enrichment genes.

Antigen-Specific T Cell Proliferation Assay. The BMDCs (BALB/c mice) were treated with 5 μ M **81**, 5 μ M **2F52** or vehicle overnight and then the BMDCs were pulsed with OVA protein or OVA₃₂₃₋₃₃₉ peptide (ISQAVHAAHAEINEAGR, InvivoGen) for 4 h. OVA₃₂₃₋₃₃₉ peptide was used as a positive control. For treatment with a mitophagy inducer, BMDCs were pretreated with 1 μ M MN58b for 1 h, then compounds were added. After washing with media, the OVA-pulsed BMDCs or nonpulsed BMDCs were cocultured with carboxyfluorescein succinimidyl ester (CFSE, Thermo Fisher Scientific, Cat#

C34554)-labeled splenic CD4⁺ T cells isolated from DO11.10 mice, which have transgenic OVA₃₂₃₋₃₃₉-specific CD4⁺ cells. After 3-d incubation, cells were stained with anti-mouse CD4 antibody (BD Biosciences) and antigen-specific CD4⁺ T cell proliferation was evaluated by CFSE fluorescence using flow cytometry. Splenic CD4⁺ T cells were isolated using EasySep Mouse CD4⁺ T cell isolation kit (negative selection) (#19852, STEMCELL Technologies). Data were analyzed using FlowJo software (FlowJo).

Assessment of Adjuvanticity of Compounds Using a Model Antigen OVA In Vivo.

For the OVA immunization model, BALB/c female mice were intramuscularly injected on days 0 and 21 with OVA protein (20 μ g per injection) plus compound (10 to 100 nmol per injection) in a total volume of 50 μ L; 10% DMSO was used as vehicle. Mice were boosted intraperitoneally on day 39 with 100 μ g per injection OVA in a total volume of 100 μ L and were bled on day 41. OVA-specific IgG1 and IgG2a levels in sera were measured by ELISA, as previously described (57). We prepared standard sera with known endpoint titers that was calculated as a reciprocal of the highest dilution that gave an absorbance reading that was double the absorbance of the background. Each ELISA plate included a titration of this standard sera to generate a standard curve. The test serum samples were tested at a 1:100 dilution and the titer was interpolated from the standard serum titration from the same plate. The results are expressed in units per milliliter (arbitrary units) and calculated based on the units per milliliter of the standard serum. In preliminary experiments to determine the optimal dose for adjuvant activity, three doses of **81** (10, 50, and 100 nmol per injection) were examined. ELISA data showed that 50 nmol per injection induced the highest antigen specific IgG2a levels (SI Appendix, Fig. S10).

Apoptosis Assay and LDH Release Detection. For apoptosis assays, BMDCs were cultured with 5 μ M **81**, **2F52** 1 ng/mL LPS, or 0.5% DMSO (vehicle) overnight. Next, 3 μ M nigericin and 50 μ M cisplatin were used as apoptosis inducers. An annexin V apoptosis detection assay was performed according to the manufacturer's protocol (BD Biosciences). To evaluate LDH release in the supernatant, THP-1 cells were treated with 5 μ M **81** or **2F52**, or 10 ng/mL LPS overnight. LDH levels in the culture supernatant were examined by the CytoTox 96 Non-Radioactive Cytotoxicity Assay (Promega). The LDH levels in a cell lysate were used as the positive control and considered as 100%. % LDH release relative to the positive control are shown.

Assessment of Local and Systemic Adverse Effects Induced by Compounds.

To analyze local adverse effects, BALB/c mice were injected with **81**, **2F52** alone (50 nmol per injection), vehicle (10% DMSO; negative control), MPLA (10 μ g per injection, InvivoGen # vac-mpla), or AddaVax (25 μ L per injection; positive control, InvivoGen #vac-adx-10) in a volume of 50 μ L. The mice were bled at 2 and 24 h and sera were assessed for cytokine/chemokine levels by multiplex cytokine assay Luminex (Thermo Fisher Scientific). CRP levels in sera were measured by ELISA. Details for antibodies are indicated in SI Appendix, Table S4. Muscles at the injected site were harvested at 24 h and histological sections with 5- μ m thickness were stained with H&E. For assessment of morbidity after administration of compounds **81** and **2F52**, C57BL/6 mice were intraperitoneally injected with 100 mg/kg liposomal formulation of compounds: 100 mg/kg (0.27 mmol/kg) **81** and 100 mg/kg (0.22 mmol/kg) **2F52**. To achieve a higher concentration, **81** and **2F52** were encapsulated into liposomes in our laboratory as previously described (58), using 1,2-dioleoyl-3-phosphatidylcholine (DOPC, Avanti polar Lipids) and cholesterol (Sigma). The compound:DOPC:cholesterol mol percent ratio was 10:80:10, respectively.

Influenza Challenge Study.

Compounds **81** and **2F52** were submitted to the Institute for Antiviral Research of Utah State University and the influenza challenge study was performed by the institute. For the influenza challenge model, antigen (A/California/07/2009 [H1N1pdm09]) was obtained from Bio-defense and Emerging Infections Research Resources Repository (BEI Resources). Influenza A/California/04/2009 (pandemic H1N1) was used for lethal challenge. Influenza A/California/04/2009 (H1N1), strain designation 175208, was received from Elena Govorkova, Department of Infectious Diseases, St. Jude Children's Research Hospital, Memphis, TN. The virus was adapted for replication in the lungs of BALB/c mice by nine sequential passages in mice. Virus was plaque purified in Madin-Darby canine kidney (MDCK) cells and a virus stock was prepared by growth in embryonated chicken eggs and then MDCK cells.

BALB/c female mice were intramuscularly injected with inactivated influenza virus (0.3 μ g per injection) plus compound (100 nmol per injection) with or without MPLA (1 μ g per injection; InvivoGen, #vac-mpla) in a 50 μ L-volume. Mice were challenged with homologous virus on day 21 after immunization and were observed for morbidity and mortality through day 21 postinfection. For challenge, mice were anesthetized by intraperitoneal injection of ketamine/xylazine (50 mg/kg/5 mg/kg) prior to challenge by the

intranasal route with $\sim 1 \times 10^5$ ($3 \times \text{LD}_{50}$) cell culture infectious doses (CCID₅₀) of virus per mouse in a 90- μL inoculum volume. Mice were weighed prior to treatment and then everyday thereafter to assess the effects of treatment on ameliorating weight loss due to viral infection.

Statistical Analysis. Data obtained in vitro studies are shown as means with SD and in vivo data are presented as means with SEM. For in vitro data, unpaired two-tailed *t* test with Welch's correction to compare two groups and one-way ANOVA with Bonferroni's or Dunnett's post hoc test were used to compare multiple groups. For comparing continuous/ordinal outcomes (antigen-specific antibodies and serum cytokine/chemokine levels) between a few groups each against a control group, Kruskal–Wallis tests with Dunn's post hoc test were applied. For body weight, a last-value carried-forward approach was used to impute missing values after a mouse was killed, the

average weight over time was used as an outcome for comparison, and one-way ANOVA with Dunnett's post hoc tests were applied. A log-rank test was used to test for a significant difference between Kaplan–Meier survival curves. Prism 5 software (GraphPad Software) was used. A *P* value less than 0.05 was considered statistically significant.

Data Availability. RNA-seq data have been deposited in ArrayExpress, <https://www.ebi.ac.uk/arrayexpress/> (accession no. E-MTAB-10269) (59). All other data are included in the manuscript and *SI Appendix*.

ACKNOWLEDGMENTS. We thank Stephen Dozier and Nina Sun for technical support in the studies using Seahorse Analyzers. This study was supported by the NIH/National Institute of Allergy and Infectious Diseases under Contracts HHSN272201400051C and 75N93019C00042 (principal investigator, D.A.C.).

1. M. M. Mosaheb, M. L. Reiser, L. M. Wetzler, Toll-like receptor ligand-based vaccine adjuvants require intact MyD88 signaling in antigen-presenting cells for germinal center formation and antibody production. *Front. Immunol.* **8**, 225 (2017).
2. S. G. Reed, M. T. Orr, C. B. Fox, Key roles of adjuvants in modern vaccines. *Nat. Med.* **19**, 1597–1608 (2013).
3. J. E. Linnik, A. Egli, Impact of host genetic polymorphisms on vaccine induced antibody response. *Hum. Vaccin. Immunother.* **12**, 907–915 (2016).
4. A. C. Shaw *et al.*, Dysregulation of human Toll-like receptor function in aging. *Ageing Res. Rev.* **10**, 346–353 (2011).
5. N. Dhiman *et al.*, Associations between SNPs in toll-like receptors and related intracellular signaling molecules and immune responses to measles vaccine: Preliminary results. *Vaccine* **26**, 1731–1736 (2008).
6. C. E. Moore *et al.*, Single nucleotide polymorphisms in the Toll-like receptor 3 and CD44 genes are associated with persistence of vaccine-induced immunity to the serogroup C meningococcal conjugate vaccine. *Clin. Vaccine Immunol.* **19**, 295–303 (2012).
7. R. Arav-Boger *et al.*, Polymorphisms in Toll-like receptor genes influence antibody responses to cytomegalovirus glycoprotein B vaccine. *BMC Res. Notes* **5**, 140 (2012).
8. E. Nanishi, D. J. Dowling, O. Levy, Toward precision adjuvants: Optimizing science and safety. *Curr. Opin. Pediatr.* **32**, 125–138 (2020).
9. G. Del Giudice, R. Rappuoli, A. M. Didierlaurent, Correlates of adjuvanticity: A review on adjuvants in licensed vaccines. *Semin. Immunol.* **39**, 14–21 (2018).
10. M. A. Lacaille-Dubois, Updated insights into the mechanism of action and clinical profile of the immunoadjuvant QS-21: A review. *Phytomedicine* **60**, 152905 (2019).
11. A. M. Didierlaurent *et al.*, Adjuvant system AS01: Helping to overcome the challenges of modern vaccines. *Expert Rev. Vaccines* **16**, 55–63 (2017).
12. P. Wang, Natural and synthetic saponins as vaccine adjuvants. *Vaccines (Basel)* **9**, 222 (2021).
13. M. Chwalek, N. Lalun, H. Bobichon, K. Plé, L. Voutquenne-Nazabadioko, Structure-activity relationships of some hederagenin diglycosides: Haemolysis, cytotoxicity and apoptosis induction. *Biochim. Biophys. Acta* **1760**, 1418–1427 (2006).
14. R. Villarreal, T. B. Casale, Commonly used adjuvant human vaccines: Advantages and side effects. *J. Allergy Clin. Immunol. Pract.* **8**, 2953–2957 (2020).
15. N. Petrovsky, Comparative safety of vaccine adjuvants: A summary of current evidence and future needs. *Drug Saf.* **38**, 1059–1074 (2015).
16. Y. J. Lin *et al.*, Oil-in-water emulsion adjuvants for pediatric influenza vaccines: A systematic review and meta-analysis. *Nat. Commun.* **11**, 315 (2020).
17. E. Tritto, F. Mosca, E. De Gregorio, Mechanism of action of licensed vaccine adjuvants. *Vaccine* **27**, 3331–3334 (2009).
18. N. M. Shukla *et al.*, Identification of compounds that prolong type I interferon signaling as potential vaccine adjuvants. *SLAS Discov.* **23**, 960–973 (2018).
19. M. Chan *et al.*, Structure-activity relationship studies to identify affinity probes in Bis-aryl sulfonamides that prolong immune stimuli. *J. Med. Chem.* **62**, 9521–9540 (2019).
20. A. Garrido, A. Lepailleur, S. M. Mignani, P. Dallelmann, C. Rochais, hERG toxicity assessment: Useful guidelines for drug design. *Eur. J. Med. Chem.* **195**, 112290 (2020).
21. T. Kawai, S. Akira, The role of pattern-recognition receptors in innate immunity: Update on Toll-like receptors. *Nat. Immunol.* **11**, 373–384 (2010).
22. J. Wu, Z. J. Chen, Innate immune sensing and signaling of cytosolic nucleic acids. *Annu. Rev. Immunol.* **32**, 461–488 (2014).
23. A. Y. Shih, K. L. Damm-Ganamet, T. Mirzadegan, Dynamic structural differences between human and mouse STING lead to differing sensitivity to DMXAA. *Biophys. J.* **114**, 32–39 (2018).
24. Z. Cheng *et al.*, The interactions between cGAS-STING pathway and pathogens. *Signal Transduct. Target. Ther.* **5**, 91 (2020).
25. A. P. West *et al.*, Mitochondrial DNA stress primes the antiviral innate immune response. *Nature* **520**, 553–557 (2015).
26. A. Dhir *et al.*, Mitochondrial double-stranded RNA triggers antiviral signalling in humans. *Nature* **560**, 238–242 (2018).
27. E. L. Mills, B. Kelly, L. A. J. O'Neill, Mitochondria are the powerhouses of immunity. *Nat. Immunol.* **18**, 488–498 (2017).
28. G. S. Shadel, T. L. Horvath, Mitochondrial ROS signaling in organismal homeostasis. *Cell* **163**, 560–569 (2015).
29. R. J. Youle, Mitochondria-Striking a balance between host and endosymbiont. *Science* **365**, eaaw9855 (2019).
30. J. X. Tan, T. Finkel, Mitochondria as intracellular signaling platforms in health and disease. *J. Cell Biol.* **219**, e202002179 (2020).
31. D. Ryu *et al.*, Urolithin A induces mitophagy and prolongs lifespan in *C. elegans* and increases muscle function in rodents. *Nat. Med.* **22**, 879–888 (2016).
32. E. Sanchez-Lopez *et al.*, Choline uptake and metabolism modulate macrophage IL-1 β and IL-18 production. *Cell Metab.* **29**, 1350–1362.e7 (2019).
33. A. P. West, G. S. Shadel, S. Ghosh, Mitochondria in innate immune responses. *Nat. Rev. Immunol.* **11**, 389–402 (2011).
34. A. Angajala *et al.*, Diverse roles of mitochondria in immune responses: Novel insights into immuno-metabolism. *Front. Immunol.* **9**, 1605 (2018).
35. A. P. West, G. S. Shadel, Mitochondrial DNA in innate immune responses and inflammatory pathology. *Nat. Rev. Immunol.* **17**, 363–375 (2017).
36. F. Hou *et al.*, MAVS forms functional prion-like aggregates to activate and propagate antiviral innate immune response. *Cell* **146**, 448–461 (2011).
37. I. A. Buskiewicz *et al.*, Reactive oxygen species induce virus-independent MAVS oligomerization in systemic lupus erythematosus. *Sci. Signal.* **9**, ra115 (2016).
38. R. B. Seth, L. Sun, C. K. Ea, Z. J. Chen, Identification and characterization of MAVS, a mitochondrial antiviral signaling protein that activates NF- κ B and IRF 3. *Cell* **122**, 669–682 (2005).
39. L. Bonifaz, M. Cervantes-Silva, E. Ontiveros-Dotor, E. López-Villegas, F. Sánchez-García, A role for mitochondria in antigen processing and presentation. *Immunology* **144**, 461–471 (2014).
40. G. Tezel *et al.*, Mechanisms of immune system activation in glaucoma: Oxidative stress-stimulated antigen presentation by the retina and optic nerve head glia. *Invest. Ophthalmol. Vis. Sci.* **48**, 705–714 (2007).
41. M. Oberkampff *et al.*, Mitochondrial reactive oxygen species regulate the induction of CD8⁺ T cells by plasmacytoid dendritic cells. *Nat. Commun.* **9**, 2241 (2018).
42. F. Y. Liew, T(H)1 and T(H)2 cells: A historical perspective. *Nat. Rev. Immunol.* **2**, 55–60 (2002).
43. T. R. Mosmann, R. L. Coffman, TH1 and TH2 cells: Different patterns of lymphokine secretion lead to different functional properties. *Annu. Rev. Immunol.* **7**, 145–173 (1989).
44. M. Redza-Dutoir, D. A. Averill-Bates, Activation of apoptosis signalling pathways by reactive oxygen species. *Biochim. Biophys. Acta* **1863**, 2977–2992 (2016).
45. K. P. Hopfner, V. Hornung, Molecular mechanisms and cellular functions of cGAS-STING signalling. *Nat. Rev. Mol. Cell Biol.* **21**, 501–521 (2020).
46. A. P. West *et al.*, TLR signalling augments macrophage bactericidal activity through mitochondrial ROS. *Nature* **472**, 476–480 (2011).
47. S. M. Wi *et al.*, TAK1-ECSIT-TRAF6 complex plays a key role in the TLR4 signal to activate NF- κ B. *J. Biol. Chem.* **289**, 35205–35214 (2014).
48. A. Matsuzawa *et al.*, ROS-dependent activation of the TRAF6-ASK1-p38 pathway is selectively required for TLR4-mediated innate immunity. *Nat. Immunol.* **6**, 587–592 (2005).
49. S. E. Weinberg, L. A. Sena, N. S. Chandel, Mitochondria in the regulation of innate and adaptive immunity. *Immunity* **42**, 406–417 (2015).
50. D. A. Sliter *et al.*, Parkin and PINK1 mitigate STING-induced inflammation. *Nature* **561**, 258–262 (2018).
51. Z. Ren *et al.*, Regulation of MAVS expression and signaling function in the antiviral innate immune response. *Front. Immunol.* **11**, 1030 (2020).
52. M. B. Lutz *et al.*, An advanced culture method for generating large quantities of highly pure dendritic cells from mouse bone marrow. *J. Immunol. Methods* **223**, 77–92 (1999).
53. S. K. Datta *et al.*, A subset of Toll-like receptor ligands induces cross-presentation by bone marrow-derived dendritic cells. *J. Immunol.* **170**, 4102–4110 (2003).
54. A. Kurimoto *et al.*, Synthesis and evaluation of 2-substituted 8-hydroxyadenines as potent interferon inducers with improved oral bioavailabilities. *Bioorg. Med. Chem.* **12**, 1091–1099 (2004).
55. T. Hayashi *et al.*, Mast cell-dependent anorexia and hypothermia induced by mucosal activation of Toll-like receptor 7. *Am. J. Physiol. Regul. Integr. Comp. Physiol.* **295**, R123–R132 (2008).
56. R. Halfmann, S. Lindquist, Screening for amyloid aggregation by semi-denaturing detergent-agarose gel electrophoresis. *J. Vis. Exp.* 838 (2008).
57. M. Chan *et al.*, Synthesis and immunological characterization of Toll-like receptor 7 agonistic conjugates. *Bioconjug. Chem.* **20**, 1194–1200 (2009).
58. F. Sato-Kaneko *et al.*, A novel synthetic dual agonistic liposomal TLR4/7 adjuvant promotes broad immune responses in an influenza vaccine with minimal reactivity. *Front. Immunol.* **11**, 1207 (2020).
59. T. Hayashi, RNA-seq of human monocytic cell line (THP-1) treated with compound 81 or vehicle controls. ArrayExpress. <https://www.ebi.ac.uk/arrayexpress/>. Deposited 18 December 2020.